

Sequential Measurement of Ascorbic Acid and Uric Acid Concentration by Linear Scan Voltammograms on The Plasma Treated Screen-Printed Carbon Paste Electrode

Yi-Huang Chang, Shih-Chang Wang, Chiun-Jye Yuan, Hung-Der Jang, Chuan-Liang Hsu, Ku-Shang Chang*

Abstract—Linear scan voltammograms of various concentrations of AA and UA was used to test the effect of screen-printed carbon electrode (SPCE) and oxygen plasma-treated SPCE's (OP-SPCE) ability to distinguish the oxidative peak potentials (E_{pa}) of UA from AA. The oxygen plasma-treated SPCE (OP-SPCE) could make the oxidative peaks of ascorbic acid (AA) and uric acid (UA) on the linear scan voltammograms became more defined with the E_{pa} to 150 mV (RSD =6.9%,n=7) and 350 mV (RSD =0.6%, n=7), respectively. While measuring a composite solution containing of AA and UA, the AA's current signals, generated at the shoulder of the AA peak curve on the linear scan voltammogram caused interference behavior thereby background currents presented to the uric acid's oxidative peak. The degree of background was found proportional to the concentration of AA in the composite solution with a linear regression equation of $y = 0.0226x + 2.421$ ($R^2=0.9962$). A sequential measurement of ascorbic acid and uric acid concentration in a composition solution by linear scan voltammograms on the plasma treated screen-printed carbon paste electrode has developed: (1) determined the AA concentration (2) determined the degree of interference caused by AA at the uric acid's oxidative peak (3) the estimated interference-free UA peak current is determined by subtracting the level of AA interference. By using the fitting procedure, The UA concentration can be quantitatively and accurately analyzed. Excellent recovery rates (97.9 to 106%) and RSD of 1.4% were obtained for the measurement of UA, even in the presence of high concentrations of AA.

Index Terms—Screen-printed carbon electrodes, Uric acid, Plasma, Ascorbic acid, Linear scan voltammograms.

I. INTRODUCTION

Uric acid (UA) is a metabolic end product of purine derivatives in the human body. The level of UA in body fluids

Yi-Huang Chang, Department of Food Science, Faculty of Health Sciences, Yuanpei University of Medical Technology, Hsinchu, 300, Taiwan
Shih-Chang Wang, Radiation Oncology Resident, Chi Mei Hospital, Tainan City...

Chiun-Jye Yuan, Department of Biological Science and Technology, National Chiao Tung University, Hsinchu, 300, Taiwan.

Hung-Der Jang, Department of Food Science, Faculty of Health Sciences, Yuanpei University of Medical Technology, Hsinchu, 300, Taiwan

Chuan-Liang Hsu, Department of Food Science, Tunghai University, Taichung 407, Taiwan

Ku-Shang Chang*, Department of Food Science, Faculty of Health Sciences, Yuanpei University of Medical Technology, Hsinchu, 300, Taiwan

(e.g. serum and urine) varies from 130 to 460 μM [1]. Elevated level of UA in body fluids could be a sign of diseases such as gout, hyperuricemia (or Lesch-Nyhan syndrome), obesity, diabetes, high cholesterol, kidney disease and cardiovascular diseases [1, 2]. Therefore, the measurement of uric acid level in body fluids is clinically valuable. Although many spectrophotometric and thermometric methods have been developed for the measurement of uric acid level in serum and urine, these methods are inconvenient due to the requirement of an extra instrumentation and are thus not suitable for point-of-care applications or home-use test systems. Uricase was used conventionally to fabricate of amperometric biosensors, used to determine the concentration of uric acid in body fluids [3]. However, strong electrochemical interference from electroactive species, such as ascorbic acid (AA), in the biological samples exposes a severe problem for their practical operation in measurement of UA concentration with a working potential of above 0.4 V.

The electrode surface was modified with a permselective polymer membrane in order to block the interfering, electroactive substances, based on their size and/or charge differences, from accessing the electrode [4]. The poly-L-lysine and poly (4-stryenesulfonate) membrane, for example, exhibits a size-exclusive permselectivity and is used to block the access of large-sized interfering electroactive substances [4]. Nafion, on the other hand, consists of a hydrophobic ($-\text{CF}_2-\text{CF}_2-$) backbone and the hydrophilic sulfonic acid ($-\text{SO}_3\text{H}$) side chains, by which the negatively-charged interfering substances may be blocked from accessing the electrode surface [5]. Although permselective polymer membranes have exhibited their ability to separate analytes from interfering electroactive substances during biosensing, they are unable to separate analytes from interfering substances of similar size and/or charges, such as in the case of AA and UA. It is difficult to eliminate the interference of AA by simply using a permselective membrane. Other materials, such as mercaptobenzimidazole [1], and glutamic acid [6], were also used to modify electrodes in order to distinguish UA from AA in a mixture composed of both substances. However, even with these modifications, interference from AA cannot be avoided when trying to detect level of UA.

Even though separation of the AA and UA peaks on the

linear scan voltammogram by modification of the electrode with nano-particle and the subsequent determination of AA and UA concentrations have been under extensive investigation by previous researches [7-11], the inference effect from AA and its impact on the estimation of UA concentration was still rarely discussed. The interference effect comes from the overlap between the oxidative potential peaks of AA and UA, generated on the same SPCE. The peak oxidative potential for AA ($AA-E_{pa}$) is usually lower than that of UA ($UA-E_{pa}$). The corresponding peak currents at various potentials were used to determine the concentrations of AA, UA, and other related compounds. However, these peak currents at $UA-E_{pa}$ are affected by the presence of AA currents, which tend to increase the background currents while determining the UA concentration. In this study, we used the oxygen plasma to treated SPCEs to enhance the electron transfer kinetics of the SPCE to UA and AA [12] and thereby minimize the degree of interference effect. Furthermore, the relationship between AA concentration and the interference at $UA-E_{pa}$ was observed to build a fitting procedure. The fitting equation was used to analyze the concentration of UA in the present of high concentration of AA.

II. EXPERIMENTAL

A. Reagents

The SPCEs were obtained from ApexBichem (Hsinchu, Taiwan). The electrodes consist of two rectangular carbon strips as the working and counter electrodes and both of these carbon electrodes with a working area of 4.8 mm^2 . Both carbon strips were printed using heat-curing carbon-composite ink. These strips were printed onto a plastic substrate, and an insulating layer served to delimit a working area and electric contacts. Ascorbic acid and uric acid were obtained from Sigma (St. Louis, MO, USA). All of the solutions were prepared with deionized distilled water (d.d. H_2O). Stock solution of $100 \text{ }\mu\text{M}$ ascorbic acid was fresh prepared in ddH_2O . Due to the low solubility, $200 \text{ }\mu\text{M}$ uric acid stock solution was freshly prepared in a $50 \text{ }\mu\text{M}$ potassium sodium phosphate buffer (pH 7.0).

B. Oxygen Plasma Treatment

The Oxygen plasma treatment was performed in a 13.56-MHz radio frequency (RF) plasma reactor designed by Branchy Technology Co. Ltd. (Tao-Yuan, Taiwan). The reactor was first evacuated to a base pressure of less than 10^{-3} Pa before the plasma gas was introduced. The SPCE was placed in the central area of the reactor, which was evacuated to a base pressure of less than 10^{-3} Pa, and plasma gas was consequently introduce into the reactor. The SPCE was then exposed to oxygen plasma under a constant system pressure of 13 Pa at a flow rate of 10 m/sec. The oxygen plasma treatment of the SPCE was performed at 100 W of plasma power for four minutes. All procedures were performed under room temperature.

C. Electrochemical Measurement

Linear scan voltammograms measurement was performed

using an electrochemical analyzer (model CHI 440, West Lafayette, IN, USA). All experiments were performed using a conventional three-electrode system, with the SPCE as the working electrode and a standard gold electrode as the counter electrode. An Ag/AgCl electrode was used as the reference electrode. Input and output signals from the potentiostat were simultaneously recorded in the personal computer. The measurements of electrodes were performed in a phosphate buffer ($100 \text{ }\mu\text{M}$, pH 7.4) without stirring. Linear scan voltammograms measurement was performed within a potential range of -0.3 and 0.7 V with a scanning rate of 50 mV/s .

Linear scan voltammograms of various concentrations of AA (0, 25, 50, 75, 100, 150, 200, $300 \text{ }\mu\text{M}$) and UA (0, 25, 50, 75, 100, 150, $200 \text{ }\mu\text{M}$) were determined. The oxidative current was calculated by subtracting the background current from the current at peak potential. To investigate the cross-talking effects of AA and UA, $100 \text{ }\mu\text{M}$ UA was paired with various concentrations of AA in composite solutions to determine the interference of UA on AA responses in linear scan voltammograms measurements. Then the interference of $100 \text{ }\mu\text{M}$ AA on the linear scan voltammograms measurements of various concentrations of UA (0, 25, 50, 75, 100, 150 and $200 \text{ }\mu\text{M}$) was investigated. The peak current of $100 \text{ }\mu\text{M}$ AA alone and the peak currents of the solutions of $100 \text{ }\mu\text{M}$ AA mixed with various concentrations of UA were compared. The relationship between the peak current (x-axis) and the concentration(s) of UA was plotted as a regression curve. The possible peak shifts, both in the x- and y-axes, caused by interferences were then determined by the regression results.

III. RESULTS AND DISCUSSION

Linear scan voltammograms of various concentrations of AA and UA was used to test the effect of oxygen plasma on the SPCE's ability to distinguish UA from AA. The linear scan voltammograms of UA and AA as measured by untreated SPCE (Fig. 1A and 1C) exhibited a broad and poorly defined oxidative peak, suggesting slow electron transfer kinetics. The peak potentials (E_{pa}) for UA and AA when measured by the untreated SPCE were 422 mV and 387 mV, respectively. The separation peak potentials (E_{pa}) between UA and AA was only 65 mV. This poorly defined oxidative peak between UA and AA by using SPCE caused the overlaps of anodic peak current (i_a) of AA and UA. When the SPCE was treated with oxygen plasma (OP-SPCE) for 4 min at the power of 100 W, the oxidative peak of UA (Fig. 1B) and AA (Fig. 1D) in linear scan voltammograms became well-defined, with the E_{pa} shifted negatively to 350 mV (RSD = 0.6%, n=7) and 150 mV (RSD = 6.9%, n=7), respectively. A marked reduction in the peak potential of AA (from 422 mV to 150 mV) indicates an improvement in the electron transfer kinetics when using the OP-SPCE. In addition, the oxygen plasma-treated SPCE (OP-SPCE) caused a noticeable improvement of SPCE electrochemical properties was also demonstrated by the fact that the anodic peak current (i_a) of AA and UA with an increase of 2-fold (Fig. 1A vs 1B and Fig.

1C vs. 1D) due to the removal of some loose lumped particles (e.g. binder) and surface contaminants (Fig. 2). The enhancement of electron transfer kinetics of the electrode to UA and AA may possibly be caused by the increase of edge planes [12,13] on the graphite particles of OP-SPCE.

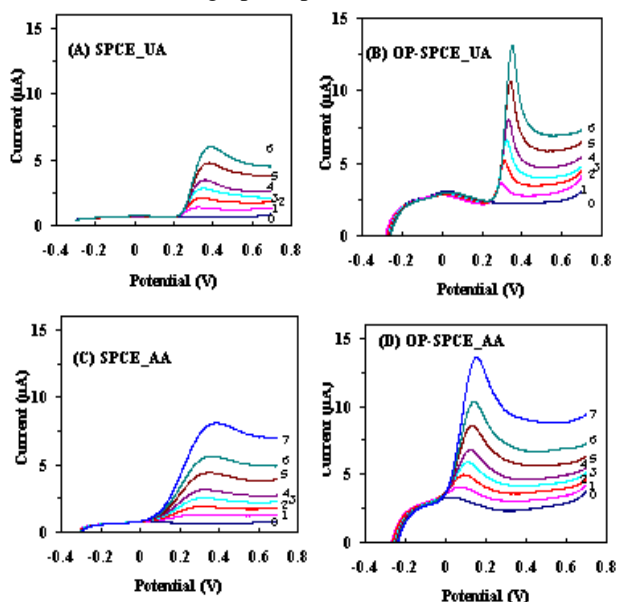


Figure 1. (A) The voltammetric scan's linear sweep of the screen-printed carbon electrode(SPCE) at various concentrations of UA; (B) The oxygen plasma treated SPCE (OP-SPCE) at various concentrations of UA; (C) SPCE at various concentrations of AA, and (D) OP-SPCE at various concentrations of AA. The CV was performed within potentials between -0.3 and 0.7 V with a scanning rate of 50 mV/s in a phosphate buffer (100 mM, pH 7.4) without stirring. (1) 0 µM, (2) 25 µM, (3) 50 µM, (4) 75 µM, (5) 100 µM, (6) 200 µM, (7) 300 µM

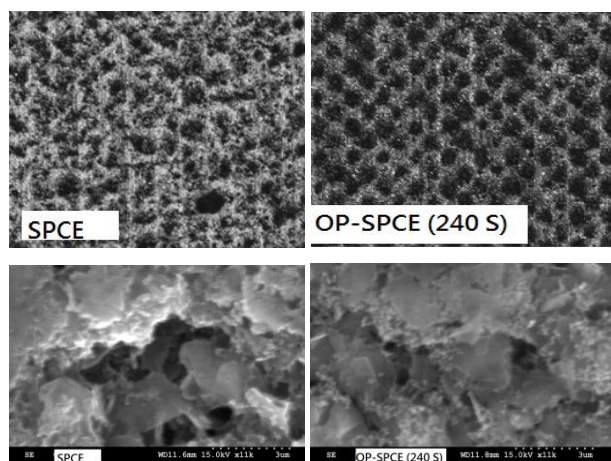


Figure 2. Light micrographs and scanning electron micrographs (SEM) of the surface of SPCEs after treating with oxygen plasma. SPCEs and SPCEs treated with oxygen plasma (OP-SPCE) prior to Light micrographs analysis (up), SPCEs and OP-SPCE s treated with oxygen plasma prior to the SEM analysis (down) . Magnification power of images is 7000X

From Fig. 1B and 1D, the oxidative currents corresponding to various AA and UA concentrations were obtained by subtracting the background currents from the peak oxidative current (*I_{pa}*) of AA and UA in their linear scan voltammograms. The obtained calibration plots for AA and UA were then determined with the regression equations summarized in Table 1, where $y = 0.0341x - 0.49$ ($R^2 = 0.9998$, Eqn(1) in Table 1) for AA and $y = 0.051x + 0.3609$ ($R^2 = 0.9981$, Eqn (2) in Table 1) for UA, with the y-axis representing the peak currents and the x-axis representing AA or UA concentrations. Both the peak currents of AA and UA increased linearly with AA and UA concentrations from 25 to 300 µM.

Table 1 Regression equations of UA and AA in the presence of interference on the OP-SPCE

	Regression Equation	R ²	Equation number
AA	$y=0.0341x - 0.49$	0.9998	(1)
UA	$y=0.051x + 0.3609$	0.9981	(2)
AA+100 µM UA	$y=0.0348x + 0.0533$	0.9995	(3)
AA's degree of interference	$y=0.0226x + 2.421$	0.9962	(4)

The determination of UA (or AA) concentration in the presence of AA (or UA) using an SPCE or OP-SPCE was carried out in mixtures containing various concentrations (25-300 µM) of UA (or AA) and fixed concentrations (100 µM) of AA (or UA) (Figure 3). As shown in Figure 3B and 3D, the oxidative peaks of AA and UA in a composite solution could be clearly distinguished with a peak separation of 200 mV when measured by OP-SPCE. In addition, when using the OP-SPCE, electrochemical responses to UA increased linearly proportionally to the concentrations of UA from 25 to 200 µM (Fig. 3B). A peak oxidative current of 6.3 µA at 150 mV for 100 µM AA could be observed in the linear scan voltammograms, with a negligible interference from UA in a range of 25-200 µM (Fig. 3B). This indicates that the peak currents of AA were not interfered with UA at various concentration of UA.

Next, the feasibility of using the OP-SPCE for the calculation of AA concentration in the presence of UA was investigated. The linear scan voltammograms plots of the composite solutions of 100 µM UA and various concentrations of AA are shown in Fig. 3D. As expected, the oxidative peak currents of AA increased linearly with respect to the AA concentration from 25 to 300 µM (Fig. 3D). A linear regression equation of the plot of oxidative peak currents vs. AA concentration was determined to be $y = 0.0348x + 0.0533$ ($R^2 = 0.9995$) in Eqn(3) in Table 1. From Eqn (1) and Eqn (3), it is observed that both the linear regression equations for the plots of oxidative peak currents vs. AA concentration with and without the presence of UA were virtually identical. This result also indicates that the peak currents of AA were not interfered with those of UA at all and the AA concentration in any composite solution

should be calculated as the first step toward determining the accurate concentrations of AA and UA.

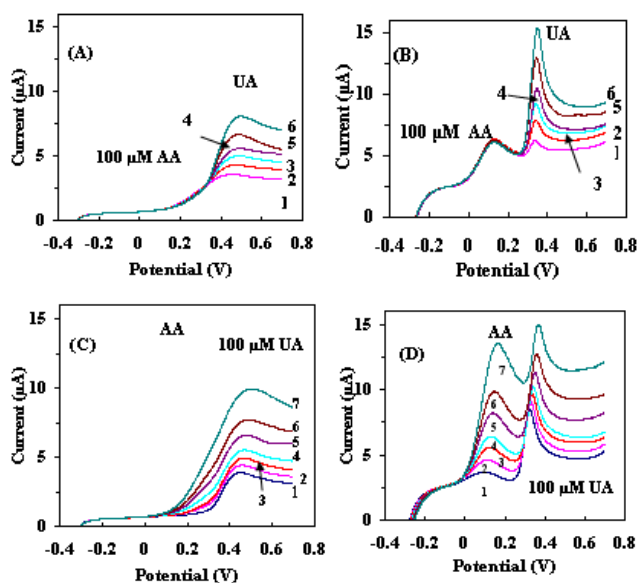


Figure 3. (A) The voltammetric scans' linear sweep of various concentrations of UA on the SPCE in the presence of 100 μM AA; (B) OP-SPCE at various concentrations of UA+100 μM AA; (C) SPCE at various concentrations of AA+100 μM UA and (D) OP-SPCE at various concentrations of AA+100 μM UA. The CV was performed within potentials between -0.3 and 0.7 V with a scanning rate of 50 mV/s in a phosphate buffer (100 mM, pH 7.4) without stirring. (1) 25 μM, (2) 50 μM, (3) 75 μM, (4) 100 μM, (5) 150 μM, (6) 200 μM, (7) 300 μM

Refer to the linear scan voltammogram plots of the composite solutions of 100μM UA and various concentrations of AA , as shown in Fig. 3D. It was found that serious interference were caused by the AA current signals generated at the shoulder of the AA peak curve on the linear scan voltammogram (Fig. 1D), which increased the background currents at UA's oxidative peak. According to Fig. 1D, the degree of interference from AA was linearly proportional to the concentration of AA with a regression equation of $y = 0.0226x + 2.421$ in Eqn(4), where y is the level of interference and x is the AA concentration. In addition, as shown in Fig. 1D, the E_{pa} of UA exhibited a slight positive shift, with respect to the AA concentration, over the range of 25-200 μM (of 20 mV/100μM). However, these shifts in the x-axis were too small to be mathematically significant (data not shown). Therefore, the second step of the analysis (Step 2 in Table 2) was to determine the degree of interference caused by AA. After the degree of interference caused by AA was calculated, the estimated interference-free UA peak current (i.e. without interference of AA) (Step 3 in Table 2) is determined by subtracting the level of AA interference. The estimated interference-free UA peak current is used at y value to solve the x value according to Eqn(2) , where x is the correct concentration of UA.

In order to check the validity of the fitting procedure presented in Table 2, a series of composite solutions of 100 μM AA and various concentration of UA (ranging from 50 to 200 μM) were created. As shown in Table 3, in the presence of 100 μM AA, recoveries of 106.1%, 104.2%, 102.6%, 98.9% and 97.9% for 50, 75, 100, 150 and 200 μM UA, respectively, were obtained by the presented method. Whereas, poor recoveries of 296.6%, 249.92%, 198.8%, 163.9% and 147.4% for 50, 75, 100, 150 and 200 μM UA, respectively when the interference effect was not taken into account. This indicates that the concentrations of AA and UA can be accurately calculated by the analysis procedure we propose in Table 2. Another series of composite solutions of 100 μM UA and various AA concentrations (ranging from 25 to 300 μM) were prepared. The solutions were analyzed with the procedure shown in Table 2, and recoveries ranging from 96% to 99% were obtained (data not shown).

Table 2 Sequential measurement of ascorbic acid and uric acid concentration concentrations in composite solutions

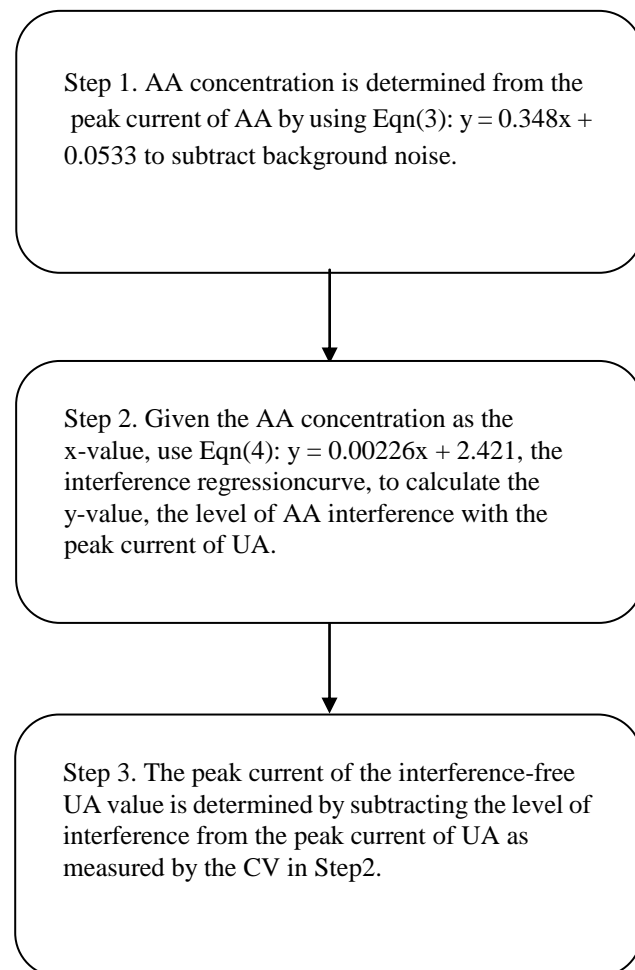


Table 3 Recovery of various concentrations of UA in the presence of 100 μM AA

UA Concentration	50	75	100	150	200
Presented method ¹					
yield	53.0	78.1	103.1	149.4	198.4
recovery	106.1	104.2	102.6	98.9	97.9
interference not taken into account ²					
yield	147.9	187.4	198.8	254.9	294.9
recovery	295.6	249.9	198.8	163.9	147.4

¹interference effect was taken into account

²interference effect was not taken into account

As shown in Fig. 4, the linear scan voltammograms of a composite solution containing both 100 μM UA and 100 μM AA in subsequent scans were similar, exhibiting oxidative peaks of 350 mV for UA and 150 mV for AA. The reproducibility of the generated OP-SPCE for analytes was also studied by successively determining the responses of 100 μM AA and 100 μM UA. The average electrochemical response of the OP-SPCE to UA and AA was 10.1 $\mu\text{A}/100 \mu\text{M}$ and 6.3 $\mu\text{A}/100 \mu\text{M}$, respectively. The relative standard deviation (RSD) for the detection of UA and AA were 1.4% and 2.2%, respectively.

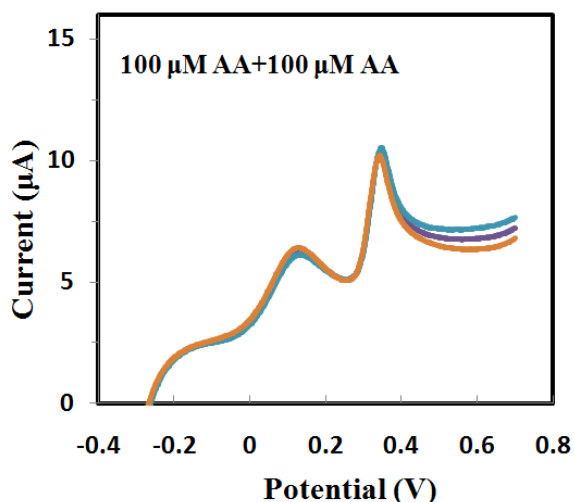


Figure 4. The voltammetric scan's linear sweep of a composite solution containing both 100 μM UA and 100 μM AA.

When measured with different OP-SPCEs, the peak currents for 25, 50, 75, 100, 150, 200 and 300 μM UA exhibited RSDs (n=3) of 13.8%, 12.3%, 12.0%, 12.0%, 11.8% and 11.7% in the linear scan voltammograms,

respectively. The poor reproducibility of preparing OP-SPCE could be caused by the organic oil and pollutants on the surface of the SPCE, incompletely cleaned by the oxygen plasma treatment. This indicates that further research are needed in order to optimize the conditions by which oxygen plasma cleans the surface of SPCEs [13].

I. CONCLUSION

This paper demonstrates that oxygen-plasma treatments can improve the separation of the ascorbic acid and uric acid oxidation peaks. Oxygen plasma treatment can not only remove the loose lumped particles (e.g. binder) and surface contaminants from the surface of SPCEs. These cleaning and modification effects of oxygen plasma caused the oxidation peaks of AA and UA in the linear scan voltammograms to become well-defined, with a peak-to-peak potential of 200 mV.

While measuring UA in a composite solution containing AA, serious interference was caused by the AA. Current signals generated at the shoulder of the AA peak curve on the linear scan voltammogram (Fig. 1D), which increased the background currents of UA's oxidative peak. Using the OP-SPCE the degree of interference from AA for the determination of UA can be reduce and has become proportional to the concentration of AA with a linear regression equation of $y = 0.0226x + 2.421$ ($R^2=0.9962$). A fitting procedure of subtracting this interference response was used to correctly analyze the concentration of UA in a composite solution. The OP-SPCE also exhibited consistency when detecting concentrations of UA and AA, with an RSD of 1.4% and 2.2%, respectively. In conclusion, we combined an effective surface-cleaning method, which improved the electrochemical properties of the SPCE, and a fitting procedure, which subtracted the interference response, to analyze the concentration of UA. It was suggested that the sequential procedure proposed provides an efficient and convenient way to solve the issue of interference responses and has great potential for determining UA concentrations in

composite solution. In the presence of a high concentration of AA (100 μ M), recoveries for UA concentrations between 50 and 200 μ M range from 106% to 97%. This range meets the clinical requirement for the abnormal elevation of UA in serum.

ACKNOWLEDGMENT

This work was financially supported by the China's (Taiwan) Ministry of Science and Technology under Project No.101-2811-M-264-002 and 107-2221-E-264-002

REFERENCES

- [1] Raj CR, Ohsaka, T. Voltammetric detection of uric acid in the presence of ascorbic acid at a gold electrode modified with a self-assembled monolayer of heteroaromatic thiol., *J. Electroanal. Chem.* 2003;540: 69–77.
- [2] Ren W, Luo HQ, Li NB. Simultaneous voltammetric measurement of ascorbic acid, epinephrine and uric acid at a glassy carbon electrode modified with caffeic acid, *Biosens. Bioelectron.* 2006; 21:1086–1092.
- [3] Kim MC, Kwal J, Lee SY. Sensing of uric acid via cascade catalysis of uricase and a biomimetic catalyst, *Sensor and Actuator B* 2016; 232: 744-749.
- [4] Yuan CJ, Hsu CL, Wang SC, Chang KS. Eliminating the interference of ascorbic acid and uric acid to the amperometric glucose biosensor by cation exchangers membrane and size exclusion membrane, *Electroanal.* 2005; 24: 2239-2244.
- [5] Don JS, Chang WB, Amperometric nitrogen dioxide gas sensor based on PAn/Au/Nafion® prepared by constant current and cyclic voltammetry methods, *Sensor and Actuator B* 2004;101:97–106.
- [6] Zhang L, Lin X. Covalent modification of glassy carbon electrode with glutamic acid for simultaneous determination of uric acid and ascorbic acid, *Analyst* 2001; 126: 367–370.
- [7] Yang Y, Jo A, Lee Y, Lee C. Electrodeposited nanoporous ruthenium oxide for simultaneous quantification of ascorbic acid and uric acid using chronoamperometry at two different potentials, *Sensor and Actuator B* 2018; 255:316-324.
- [8] Wang Z, Guo H, Gui R, Jin H, Zhang F. Simultaneous and selective measurement of dopamine and uric acid using glassy carbon electrodes modified with a complex of gold nanoparticles and multiwall carbon nanotubes, *Sensor and Actuator B* 2018; 255: 2067-2077.
- [9] Yadav DK, Gupta R, Ganesan V, Sonkar PK. Individual and simultaneous voltammetric determination of ascorbic acid, uric acid and folic acid by using a glassy carbon electrode modified with gold nanoparticles linked to bentonite via cysteine groups, *Microchim Acta* 2017;184: 1951–1957.
- [10] Li Y, Lin H, Peng H, Qi R, Luo C.. A glassy carbon electrode modified with MoS₂ nanosheets and poly(3,4-ethylenedioxythiophene) for simultaneous electrochemical detection of ascorbic acid, dopamine and uric acid, *Microchim Acta* 2016; 183: 2517–2523.
- [11] Nikos G, Tsierkezos NG, Othman SH, Ritter U, Hafermann L, McCarthy EK. Electrochemical analysis of ascorbic acid, dopamine, and uric acid on noble metal modified nitrogen-doped carbon nanotubes, *Sensor and Actuator B* 2016; 231: 218-229.
- [12] Stamatin SN, Hussainova I, Ivanov R, Colavita PE. Quantifying graphitic edge exposure in graphene-based materials and its role in oxygen reduction reactions, *ACS Catal.* 2016; 6: 5215–5221.
- [13] Wang SC, Chan g KS, Yuan CJ. Enhancement of electrochemical properties of screen-printed carbon electrodes by oxygen plasma treatment, *Electrochim. Acta* 2009; 54: 4937–4943.

Dr. Ku-Shang Chang received his PhD degree in Microbiological and Biological Engineering from the National Taiwan University, Taipei, Taiwan. He is currently a professor in the Department of Food Science at Yuanpei University of Medical Technology, Hsinchu City, Taiwan. His research interest is in development of chemical sensor and biosensor.

Dr. Yi-Huang Chang received his MSc and PhD degree in Food Engineering from the University of Wisconsin-Madison, USA. He is currently an associate professor in the Department of Food Science at Yuanpei University of Medical Technology, Hsinchu City, Taiwan. His research interest is in food chemistry and food engineering.

Dr. Shih-Chang Wang received his Ms degree in Department of Biological Science and Technology, National Chiao Tung University, Hsinchui, Taiwan and Graduated from Kaohsiung Medical University, Faculty of Medicine. He is currently a resident doctor in Chi Mei Hospital, Tainan, Taiwan. His research interests include life science, chemical sensors, tumor physics and tumor biology

Chiun-Jye Yuan received his PhD degree in Life Science from Iowa State University, USA. He is currently a professor in Department of Biological Science and Technology, National Chiao Tung University, Hsinchui, Taiwan. His research interests include life science and chemical sensor.

Dr. Hung-Der Jang received his MSc (1992) and PhD (1996) degree in Agricultural Chemistry from the National Taiwan University, Taipei, Taiwan. He is currently a professor in the Department of Food Science at Yuanpei University of Medical Technology, Hsinchu City, Taiwan. His present research interest is in fermentation technology and food microbiology.

Dr. Chuan-Liang Hsu received his PhD degree in Biological Engineering from the University of Missouri-Columbia in 1998. He is currently a professor in the Department of Food Science at Tunghai University, Taichung City, Taiwan. His research interest is in food and bio-materials process engineering and analytical chemistry.